



UNIVERSIDADE ESTADUAL DE CAMPINAS
SISTEMA DE BIBLIOTECAS DA UNICAMP
REPOSITÓRIO DA PRODUÇÃO CIENTÍFICA E INTELLECTUAL DA UNICAMP

Versão do arquivo anexado / Version of attached file:

Versão do Editor / Published Version

Mais informações no site da editora / Further information on publisher's website:

<https://www.sciencedirect.com/science/article/pii/S0261306914001344>

DOI: 10.1016/j.matdes.2014.02.026

Direitos autorais / Publisher's copyright statement:

©2014 by Elsevier. All rights reserved.

DIRETORIA DE TRATAMENTO DA INFORMAÇÃO

Cidade Universitária Zeferino Vaz Barão Geraldo

CEP 13083-970 – Campinas SP

Fone: (19) 3521-6493

<http://www.repositorio.unicamp.br>



Microstructure, phases morphologies and hardness of a Bi–Ag eutectic alloy for high temperature soldering applications



José Eduardo Spinelli^{a,*}, Bismarck Luiz Silva^a, Amauri Garcia^b

^a Department of Materials Engineering, Federal University of São Carlos, UFSCar, 13565-905 São Carlos, SP, Brazil

^b Department of Materials Engineering, University of Campinas, UNICAMP, PO Box 6122, 13083-970 Campinas, SP, Brazil

ARTICLE INFO

Article history:

Received 7 November 2013

Accepted 11 February 2014

Available online 18 February 2014

Keywords:

Solidification
Microstructure
Bi–Ag alloys
Hardness
Solders

ABSTRACT

The conversion to RoHS-compliant lead-free assembly has been a considerable challenge to the electronics industry. Among several alternative solder alloys, Bi–Ag alloys have been highlighted as a potential candidate to replace high Pb solder alloys for applications in oil and gas, automotive and avionics industries. The typical melting temperatures of Bi–Ag near-eutectic alloys are considered acceptable and excellent mechanical properties may be achieved with appropriate microstructures. Such promising alloys for high temperature soldering remain barely understood especially regarding non-equilibrium solidification features. In this study, a directional solidification experiment was carried out with the Bi–2.5 wt%Ag eutectic so that a large range of cooling rates (\dot{T}) could be obtained under unsteady-state conditions. The experimental investigation include: thermal solidification parameters (growth rate, v and cooling rate, \dot{T}), microstructure parameters (eutectic/dendritic spacing, interphase spacings) and phases morphologies analyzed by optical microscopy, scanning electron microscopy (SEM), energy-dispersive X-ray spectroscopy (EDS), and hardness. Experimental interrelations between hardness and microstructure (scale and morphology) of the eutectic Bi–Ag are reported. Solidification parameters are also associated with each configuration observed along the casting, i.e., coexistence of dendrites and eutectic cells for regions very close to the cooled casting surface, eutectic cells prevailing and eutectic cells together with β -Bi primary phase. The cell spacing, λ_c , is correlated with hardness by Hall–Petch type equations.

© 2014 Elsevier Ltd. All rights reserved.

1. Introduction

In the last years it is noted an increase in the number of restrictions proposed with a view to minimizing the use of Pb in the electronics industry, which justify the need for alternative Pb-free solder alloys. According to a survey conducted by Normann [1] interviewing application engineers, the temperature range in which electronics devices have to operate reliably is 150–250 °C. The temperature of solder joints in service are only appropriate if lower than the *solidus* or eutectic temperatures. Bi–Ag is a eutectic system in which the eutectic reaction occurs at about 2.5 wt%Ag and 262.5 °C. In this case, near eutectic Bi–Ag alloys become very promising solder alternatives when considering the melting point. Indeed, the temperature criterion is obviously not enough to guarantee soundness for a candidate alloy for replacing high Pb-alloy solders. However, Bi is the least toxic of the heavy metals, which allows its application as a substitute for Pb becoming a step toward an environmentally friendly soldering technique.

Some of the promising candidates on replacing of high Pb solders derive from the Au–Sn, Au–Ge, Zn–Al, Zn–Sn, Bi–Ag and Sn–Sb alloy systems [2]. The Bi–2.5Ag alloy is considered an interesting option due to compatible melting point and hardness if compared with Pb-based traditional solder alloys, with an actual possibility of having ductility increased. As a consequence, a Bi–Ag alloy has already been developed as a die attach solder for power devices and light-emitting diodes (LEDs) [2]. Au–Ge-based alloys have also been proposed as possible high-temperature lead-free solder materials for highly loaded components such as high-power microelectromechanical systems (MEMS) devices [3]. Nowadays, few candidates have been proposed for high-temperature lead-free solder application, such as Au–(Sn, Si, Ge), Bi–Ag, and Zn-based alloys. Au- and Bi-based alloys face several serious problems such as high costs and massive intermetallic compound (IMC), which are naturally brittle [4–6]. In solder alloys application, the ability of a liquid alloy to flow or spread on the substrate is crucial for the formation of a metallic bond driven by the physico-chemical properties of the liquid solder/solid substrate system [6].

* Corresponding author. Tel.: +55 16 3351 8512; fax: +55 16 3361 5404.

E-mail address: spinelli@ufscar.br (J.E. Spinelli).

Two fundamental aspects deserve attention considering the development of Bi–Ag alloys for soldering processes, which are the effects of the cooling rate variation on the final solder fillet microstructure and the possibility of improving properties by both adding Ag and controlling the final configuration of Bi-rich and Ag-rich phases looking for an optimized arrangement. None of these aspects is completely understood for alloys of interest on the Bi–Ag system. In this context, unidirectional solidification systems can be very useful for investigating the evolution of microstructures in solder alloys.

In the Bi–Ag system, the equilibrium eutectic mixture is formed by a solid solution of Bi in Ag on the Ag-rich side and the almost pure Bi-phase on the Bi-rich side. However, non-equilibrium solidification structural features for Bi–Ag alloys have been identified by Song et al. [7,8]. The eutectic Bi–2.5 wt%Ag sample was obtained by a gravity-casting technique without any monitoring of temperature evolution during solidification [7]. Eutectic cells comprising extremely fine Ag-rich nodules have been reported with some larger Ag particles located close to the eutectic cell boundaries. Some regions characterized by Bi grains and few primary Ag particles have also been reported. In the case of rapidly solidified Bi–2.5 wt%Ag solder pellets by arc melting, Song et al. [8] identified a microstructure consisting of coarse Bi and fine Bi–Ag eutectics.

Mechanical properties play an important role on the final characteristics of solder alloys. For instance, it is desirable a combination of low yield strength and high ductility with a view to ensuring that the solder could be extruded in wires, which are commonly used in automated soldering processes [9]. If a dendritic solder fillet microstructure is developed, properties like mechanical strength and ductility may be directly influenced by the scale and continuity of the dendritic primary branches, while the spacing between secondary arms can effectively serve to isolate a complex dispersion of second phases having a significant contribution to the mechanical properties. It is well known that the scale of the microstructural patterns, characterized by cellular, dendritic or interphase spacings, can significantly affect the properties of as-cast, heat treated and mechanically worked metallic components [10–14].

The tensile behavior of Bi–Ag alloys is reported in the literature for two distinct chemistries, i.e., Bi–2.5 and 11.0 wt%Ag [8]. The increase in the alloy Ag content is reported to increase both the yield and ultimate tensile strengths. In the case of the eutectic Bi–2.5 wt%Ag alloy the average ultimate tensile strength remained around 30 MPa with some variation depending on the adopted strain rate. The ductility is also reported to increase with the increase in Ag content with the elongation-to-fracture increasing remarkably from 4% to 38%, for 2.5 and 11%Ag, respectively. Considering that Ag hardness is lower than Bi hardness [15], the massive presence of Ag-rich particles may explain such behavior according to the authors, who state that the ductile Ag phase can accommodate the stress intensity retarding strain localization, and as a consequence improving ductility. The results shown by Masayoshi and co-authors [16] corroborate the aforementioned results with gradual increase in the tensile strength with the increase in the alloy Ag content. In this study, the dispersed Ag phase with average size of 18 μm is reported to act as an effective arrester against propagating cracks. Further, it is stated that the microstructure of the Bi–2.5wt%Ag solder alloy do not depend on the cooling rate since the microstructure of a quenched sample was considered quite similar to that of a air-cooled one [16].

According to Kim et al. [17], although the Vickers microhardnesses of Bi–2.5 and 5.0 wt%Ag alloys are fairly similar to that of a Pb–5 wt%Sn alloy, these Bi–Ag alloys exhibited a brittle behavior when compared with that of the high-Pb solder. The reported hardness values were 8.9 (± 0.17) HV, 15.0 (± 0.99) HV and 15.2 (± 2.5) HV for the Pb–5 wt%Sn, Bi–2.5 wt%Ag and Bi–5.0 wt%Ag alloys, respectively.

The present article focuses on the monitoring and characterization of a Bi–2.5 wt%Ag alloy casting directionally solidified under a wide range of cooling rates. The aim is to correlate the microstructural pattern with the experimentally determined solidification thermal parameters such as the growth rate and the cooling rate. Experimental growth laws interrelating cell spacing, interphase spacing and Ag-rich spheroid diameter with thermal parameters are also envisaged. Finally, complementary results such as the segregation profile of silver and hardness indentations are intended to be correlated with the scale and morphology of the phases forming the Bi–2.5 wt%Ag solder microstructure.

2. Experimental procedure

In order to promote growth of solidification microstructures under a wide range of cooling rates, heat was directionally extracted only through a water-cooled bottom made of low carbon steel. Further details about the solidification system used in the present research have been described in a previous study [12]. The Bi–2.5 wt%Ag alloy was melted in situ by controlling the power of the radial electrical wiring. The electric heaters were disabled so that solidification could be initiated, and at the same time the controlled water flow was initiated. Continuous temperature measurements in the casting were performed during solidification by fine type J thermocouples (0.2 mm diameter wire sheathed in 1.0 mm outside diameter stainless steel tubes) placed along the casting length. The eutectic temperature of the Bi–2.5 wt%Ag alloy is 262.5 °C.

The data acquisition system employed allows accurate determination of the slope of the experimental cooling curves. Hence, the cooling rate of the eutectic front has been determined by considering the thermal data recorded immediately after the passage of the eutectic front by each thermocouple.

An etching solution of 96% (vol.) $\text{C}_2\text{H}_5\text{OH}$ and 4% (vol.) HNO_3 applied during 30 s was used to reveal the microstructures. Deep etching procedures were performed up to 2 min which was enough to partially dissolve the β -Bi matrix and the β -Bi phase of the eutectic mixture, preparing adequate sample for SEM. The primary dendrite arm spacing and the cell spacing (λ_1) were measured on transverse sections of the casting. The triangle method was used in order to perform such measurements [18]. Further, the intercept method was adopted (also on transverse specimens) in order to determine the interphase spacing (λ), which is in brief the distance between two adjacent Ag spheroids positioned side by side inside the eutectic mixture. Image processing systems were used to measure the cited spacings and their distribution ranges. At least 30 measurements were performed for each selected position. Microstructural characterization was completed using a Field Emission Gun (FEG) – Scanning Electron Microscope (SEM–EDS) Philips (XL30 FEG).

Before hardness tests the specimen surfaces were polished with fine sandpaper to remove any machining marks. Vickers microhardness tests were performed on the cross sections of the samples by using a test load of 500 g and a dwell time of 15 s. Other hardness measurements were carried out using a Brinell hardness tester, applying a steel ball of 2.5 mm diameter and a load of 5 kg for 30 s. The adopted hardness value of a representative position was the average of at least 10 measurements on each sample and on each hardness test. Samples for segregation analysis underwent a fluorescence spectrometer (FRX), model Shimadzu EDX-720 to estimate local average concentration through an area of 100 mm^2 probe.

3. Results and discussion

Fig. 1 shows the macrograph that resulted after chemical etching performed on the entire longitudinal section of the directionally solidified Bi–2.5 wt%Ag alloy casting. Fine columnar grains

grew from the bottom towards the top of the casting, with coarser grains observed in the final third part of the mentioned casting. Well-aligned grains along the heat flow path, as can be seen in Fig. 1, allow a very comprehensive determination of microstructural parameters to be done. In the present study the parameters to be determined are the cellular spacing or the primary dendritic spacing (λ_1), and the interphase spacing (λ).

The evolution of temperature along the casting length, as a function of time, was acquired during growth of the aforementioned casting, as shown in Fig. 2. The experimental cooling curves refer to thermocouples located at specific distances from the cooled surface. The eutectic temperature is also indicated in Fig. 2a. The thermal readings have been used to provide a plot of position from the metal/mold interface and the corresponding time of the eutectic front passing by each thermocouple. The derivative of this function with respect to time gave values for the growth rate (v), as shown in Fig. 2b. The experimental tip cooling rate (\dot{T}) along the casting length is shown in Fig. 2c. The experimental tendencies inserted in Fig. 2b and c allow sustaining that a limited range of growth rate values was attained while a large spectrum of cooling rates can be seen. For instance, the growth rate associated with the relative distances from the cooled surface 10 mm and



Fig. 1. Columnar growth developed during the upward directional solidification of the eutectic Bi–2.5 wt%Ag solder alloy.

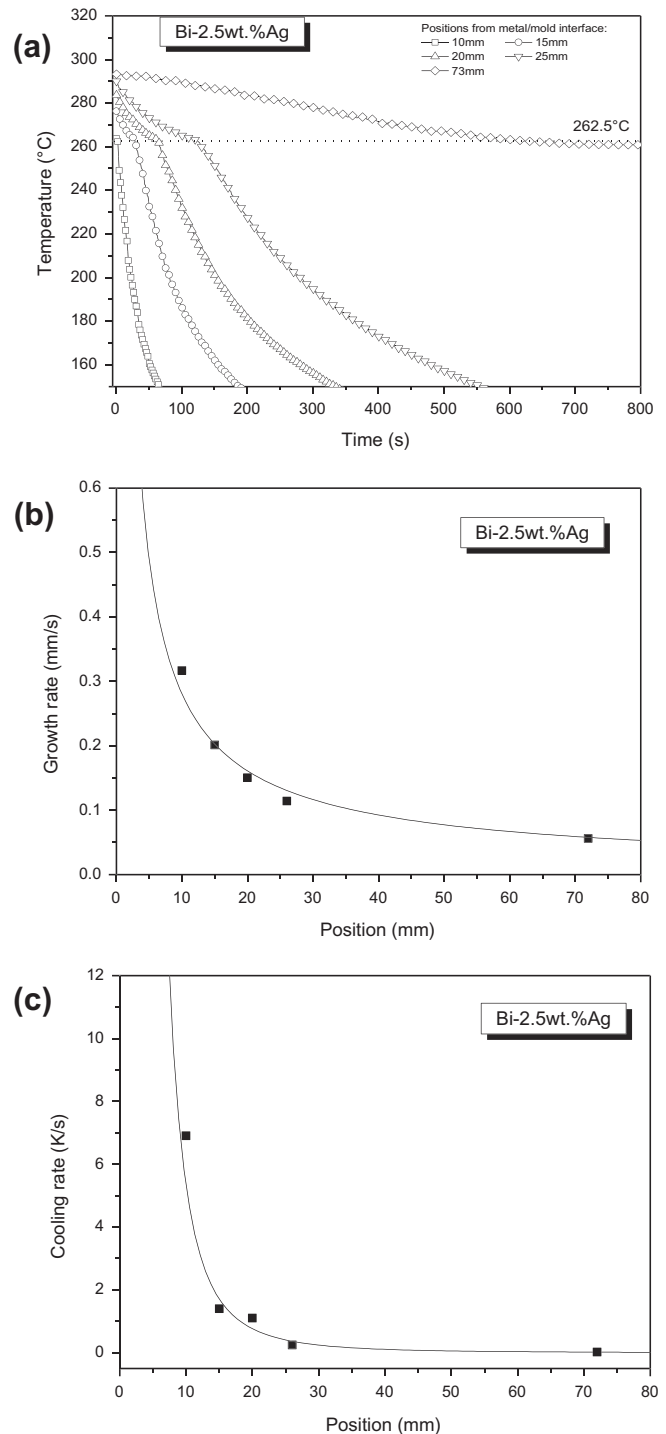


Fig. 2. (a) Cooling curves acquired for the Bi–2.5 wt%Ag alloy at different positions from the cooled bottom of the casting; (b) experimental growth rate as a function of position; and (c) cooling rate against position.

73 mm are 0.32 mm/s and 0.06 mm/s, respectively. On the other hand, the experimental cooling rates corresponding to the same mentioned positions are 7.0 K/s and 0.03 K/s.

Typical longitudinal and transverse microstructures shown in Fig. 3 aid to elucidate the changes that occurred on both the morphology and the scale of the microstructure along the casting length. From Fig. 3a–d the relative position associated with specimens subjected to optical microscopy becomes increasingly farther from the cooled surface of the Bi–2.5 wt%Ag alloy casting, i.e.,

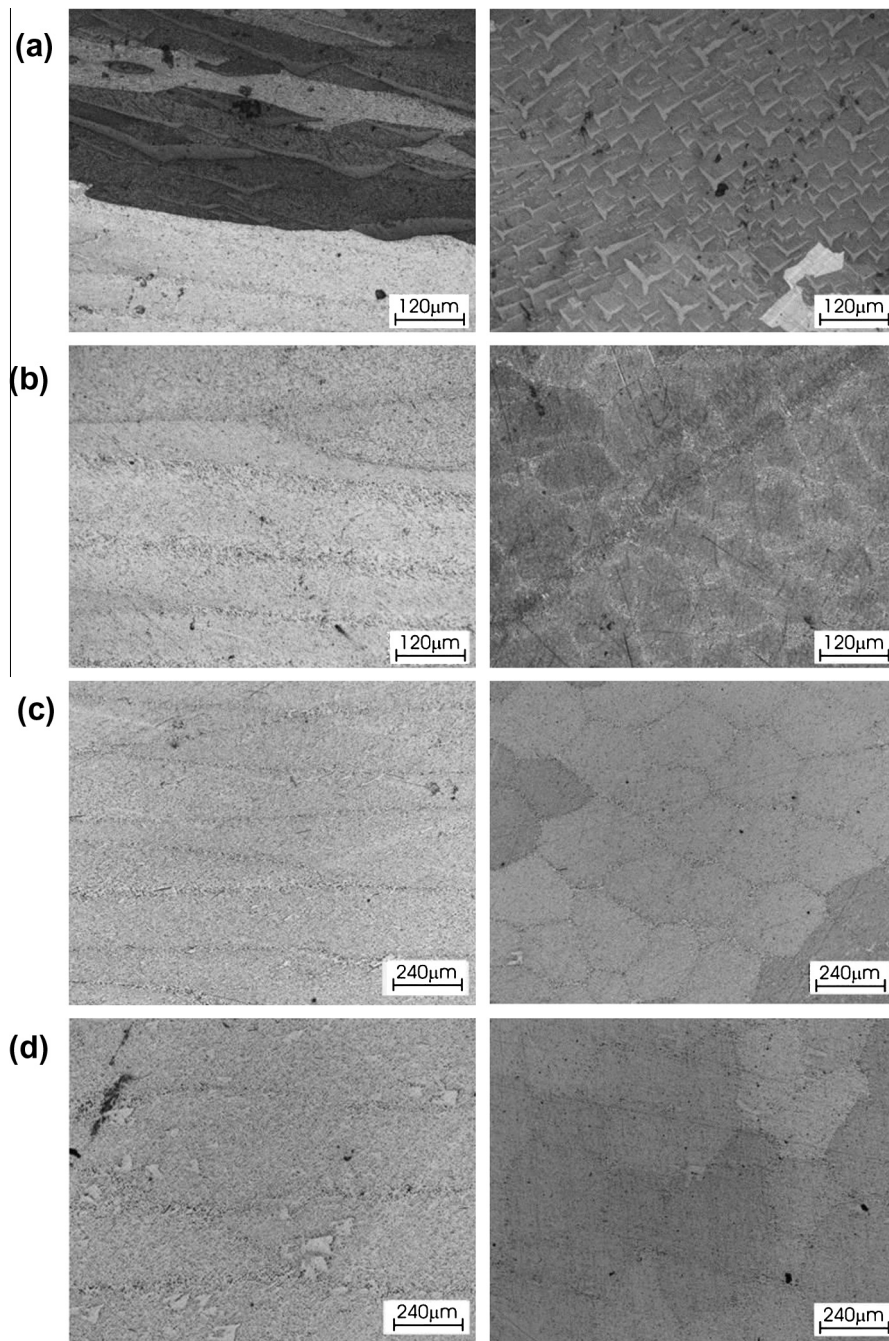


Fig. 3. Representative longitudinal (left images) and transverse (right side) microstructures of the directionally solidified Bi–2.5 wt%Ag alloy casting (a) $P = 5$ mm, $v = 0.50$ mm/s, $\lambda_1 = 54$ μm ; (b) $P = 10$ mm, $v = 0.30$ mm/s, $\lambda_1 = 113$ μm ; (c) $P = 30$ mm, $v = 0.11$ mm/s, $\lambda_1 = 255$ μm and (d) $P = 50$ mm, $v = 0.07$ mm/s, $\lambda_1 = 289$ μm . P is the position from the metal/mold interface, v is the growth rate and λ_1 is the average cell spacing or the average primary dendritic spacing.

$P = 5$ mm (Fig. 3a); $P = 10$ mm (Fig. 3b); $P = 30$ mm (Fig. 3c) and $P = 50$ mm (Fig. 3d). The distinct microstructural length scales are mainly connected with the experimental cooling rates, which are high close to the bottom of the casting, decreasing toward the top (see Fig. 2c).

Other transverse microstructures observed along the casting length are shown in Fig. 4 so that the morphological transitions could be emphasized. An abrupt cellular to dendritic transition occurred. Dendrites have prevailed for experimental growth rates higher than 0.50 mm/s. The same “ v ” value was recently reported concerning the same kind of transition observed during directional solidification of the eutectic Sn–0.7 wt%Cu solder [19].

After the region with prevalence of dendrites, the eutectic Bi–2.5 wt%Ag alloy grows with a cellular pattern, as shown in Figs. 3 and 4. These eutectic two-phase cells are also known as eutectic colonies. This kind of structure is hardly seen in the equilibrium solidification of binary eutectic alloys, however, solute impurities and non-equilibrium solidification conditions can promote instability at the planar eutectic interface resulting in the formation of two-phase eutectic colonies [20]. After the growth of cells is established, the presence of a small number of particles covering the microstructures can be noted either on longitudinal or on transverse samples. This starts to happen around the position $P = 30$ mm from the metal/mold interface, which corresponds to

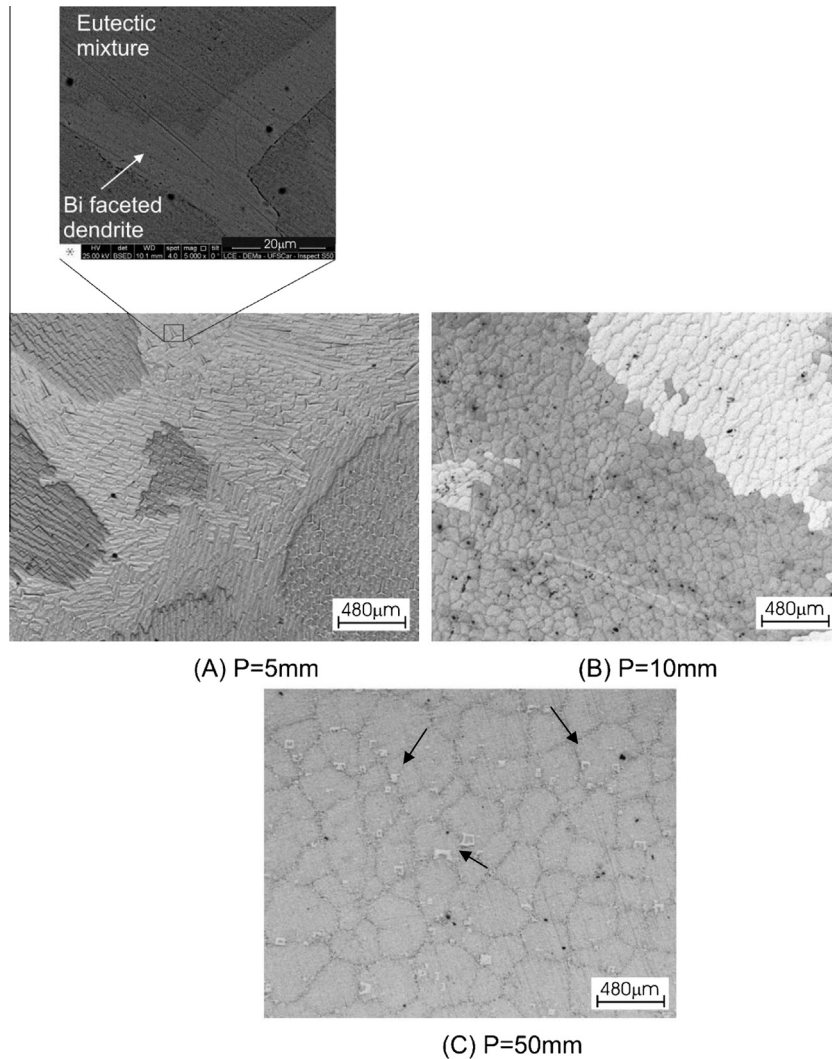


Fig. 4. Transverse sections of samples detailing the different morphologies found for the Bi–2.5 wt%Ag alloy: (A) Faceted dendrites; (B) eutectic colonies and (C) eutectic colonies together with the faceted Bi-rich precipitates (signalized with the arrows). P is the position from the metal/mold interface.

an experimental growth rate of 0.11 mm/s. Further, lower growth rates have induced considerable increase in the number of small particles disseminated throughout the microstructure (see Fig. 4). The elemental maps provided by the SEM–EDS proved that such particles are Bi-rich ones as can be seen in detail in Fig. 5.

According to Song et al. [21] Bi–Ag alloys exhibit a non-equilibrium eutectic solidification feature, which denotes that the investigation and the characterization of such eutectic system may become very important due to its anomalous broken appearance. Such authors argue that a longer solidification period involving temperatures just above the eutectic point contributes to a more faceted character of the primary Ag. However, the microstructures of the eutectic Bi–2.5 wt%Ag alloy samples solidified under very slow cooling rates (in the range 0.017–0.25 K/s) are characterized practically by absence of faceted Ag with some large primary Ag plates originated by heterogeneous nucleation, since the solidification of very small pellets (diameter < 3.0 mm) was carried out considering the mentioned thermal processing conditions. In general, eutectic cells comprising extremely fine Ag-rich nodules can be observed with a small number of Bi grains appearing occasionally.

The observed features by Song et al. [21] seem to encompass the directionally solidified microstructures observed in the present

investigation especially regarding to the slow-cooled regions of the directionally solidified Bi–Ag casting, which means cooling rates lower than 0.20 K/s corresponding to $P > 30$ mm (Figs. 3c and d and 4c). A fully dendritic arrangement can be observed in Fig. 3a with light regions constituted by the primary solid formed, which is a Bi-rich β phase and a eutectic mixture represented by the dark interdendritic regions.

Bi-rich phases present in both regions, i.e., very close to the cooled surface as dendrites and farther from such region as isolated particles, seem to grow with a faceted interface as can be seen in the inlet image of Fig. 4a. The primary Bi particles showed internal branching and faceted contours ($v < 0.11$ mm/s). This means that Bi is growing in a faceted manner, which is in disagreement with previous studies and calculations [22,23]. Such studies were carried out following quasi-stationary heat flow regimes of solidification, with samples being maintained during long periods through a temperature region above the *liquidus* temperature or the eutectic point. It seems that the transitory heat flow conditions provided in our experiment associated with high cooling rates allowed that Bi may develop a tendency to become faceted.

The average eutectic cell spacing was found to vary between 113 μ m and 351 μ m and the average interphase spacing associated

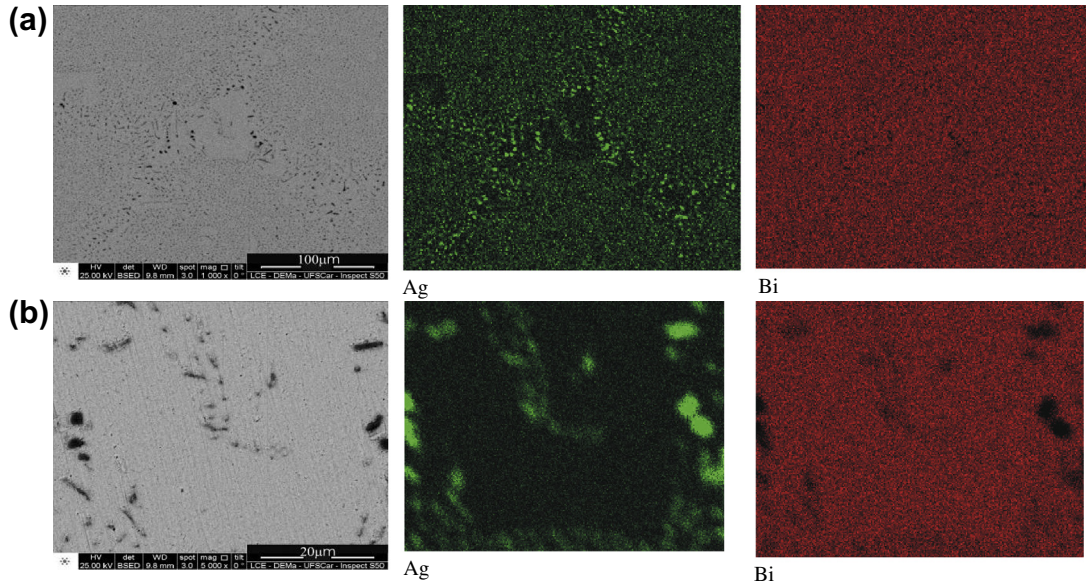


Fig. 5. Elemental SEM-EDS mappings obtained along the transverse specimen at the position $P = 50$ mm from the metal/mold interface of the vertically solidified Bi-2.5 wt%Ag solder alloy casting: (a) Magnification 1000 \times and (b) magnification 5000 \times . The digital images were acquired by SEM, using the backscattering-mode.

with the presence of Ag-rich spheroids in the eutectic colonies were in the range 0.4–1.7 μm .

Dotted regions observed in Fig. 5 reveal the arrangement of the eutectic mixture, which is quite regular along the entire Bi-2.5 wt%Ag alloy casting. On the other hand, the smooth areas correspond to the Bi-rich particles. The eutectic is formed by solid solution of Bi in Ag on the Ag-rich side and by an almost pure Bi-phase on the Bi-rich side. Although the eutectic arrangement (size, morphology and distribution) is considered a key factor controlling soundness of a solder fillet, studies dealing with such features on Bi-Ag alloys are scarce in the literature. Hence, there is a clear need for establishing the influence of the solidification thermal parameters such as the cooling rate and the tip growth rate on the final Bi-Ag solder microstructure. This is due to the fact that the resulting microstructure totally depends on the thermal processing variables imposed during the soldering process or thermal cycling.

Contrasting with single-phase cells and dendrites, there is limited examination of the dependence of growth rate of eutectic cells and dendrites on the spacing, morphology, and spatial distribution of phases forming the eutectic mixture. Different interrelations between eutectic cells/dendrites and growth rates are affirmed by Tewari et al. [20], with lower exponents characterizing power growth laws if compared with those generally adopted for the growth of single-phase cells and dendrites. The exponents -1.1 and -0.55 have been found to apply for power growth laws concerning the growth rate ($\lambda_1 = A (\nu)^{-1.1}$) and the cooling rate ($\lambda_1 = B(\dot{T})^{-0.55}$), respectively, and are the same employed with good consistency in previous studies devoted to the growth of microstructures of single-phase alloys [24].

The cell spacing and primary dendrite arm spacing have been measured along the casting length. In order to permit a correlation between these microstructural spacings and solidification thermal parameters to be established, their average, minimum and maximum values are plotted as a function of both tip cooling rate and growth rate in Fig. 6. Following the bases adopted by Tewari et al. [20], the power-function exponents traditionally used for single-phase growth cannot be applied to the growth of a directionally solidified eutectic Bi-2.5 wt%Ag solder alloy under unsteady-state heat flow conditions. The adopted exponents are $-1/2$ and $-1/4$ for the growth rate and the cooling rate, which

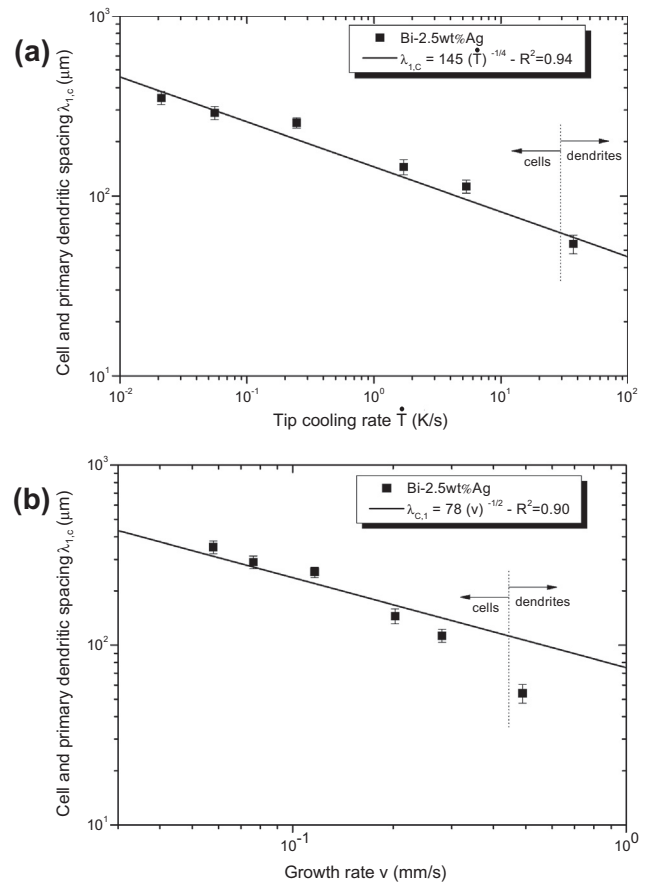


Fig. 6. Eutectic cell and primary dendritic spacings as a function of (a) tip cooling rate and (b) growth rate for a Bi-2.5 wt%Ag alloy. R^2 is the coefficient of determination.

are not able to encompass both cellular and dendritic regions. For a specific cooling rate, the corresponding experimental point associated with the eutectic dendritic growth is reasonable far from the implemented tendency (Fig. 6b).

The experimental setup used in the present study is designed for transient solidification under a range of relatively high cooling rates and growth rates. On the other hand, lower range of growth rates could be typically obtained during Bridgman-type steady state solidification tests. In steady-state growth experiments, solidification is highly controlled and the significant controllable thermal variables, the thermal gradient (G) and the growth rate (v), are maintained constant and are practically independent of each other. In transient solidification experiments (present study), these variables are interdependent, cannot be controlled and vary freely with time. The tip cooling rate synthesizes these two variables, since $\dot{T} = G \cdot v$. In a recent study on the cellular growth of Zn–Cu alloys in the same experimental set-up used in the present study, it has been shown that an equation relating the cellular spacing to the cooling rate, derived for transient solidification, has been shown also to be able to represent the cellular experimental scatter of steady-state experiments, i.e., even under a lower range of growth rates at a relatively high constant thermal gradient of 15 K/mm. So, our expectation is that the equation proposed in Fig. 6a will also encompass cases of lower growth rates.

Typical cooling rates during reflow procedures in industrial practice remain between 3.0 and 10.0 K/s. Part of the present experimental results is associated with the same order of magnitude of cooling rates since our experimental cooling rate range is from 0.05 to 37.0 K/s. This indicates that results from the directional solidification setup have a correspondence with the industrial procedures.

Fig. 7a shows the evolution of the eutectic interphase spacing along the Bi–Ag alloy casting encompassing both cellular and dendritic regions. The experimental average values are plotted along with the standard deviations. Finer Ag spheroids are associated with regions close to the casting cooled surface as shown in terms of the particle diameter in Fig. 7b. A single experimental eutectic growth law encompasses both regions experimentally examined. The eutectic growth complied with the classical relationship for lamellar eutectic growth proposed by Jackson and Hunt, with a power function exponent of $-1/2$ [25].

Fig. 7 depicts detailed SEM images, which can elucidate some microstructural features observed and discussed up to now. Fig. 7(a) shows some formation of strings of Ag spheroids, which occurred preferentially for lower growth rates.

Fig. 8 shows the results of hardness tests as a function of the cell/dendritic spacing separated in two hardness types. Vickers microhardness may represent a local measurement while the Brinell test allows bigger impressions to be formed on the surface of a specimen which can be more representative of the ensemble of microstructural features found along the Bi–2.5 wt%Ag alloy casting. Both procedures are considered complementary. Classical Hall–Petch relationships are able to represent the hardness behavior for both Brinell and Vickers procedures. The coefficients of determination, R^2 , have been inserted in order to indicate the strength of the linear relationships between the two variables. The alloy hardness increases with the decrease in the primary dendritic arm spacing or cell spacing. On the other hand, it can be seen

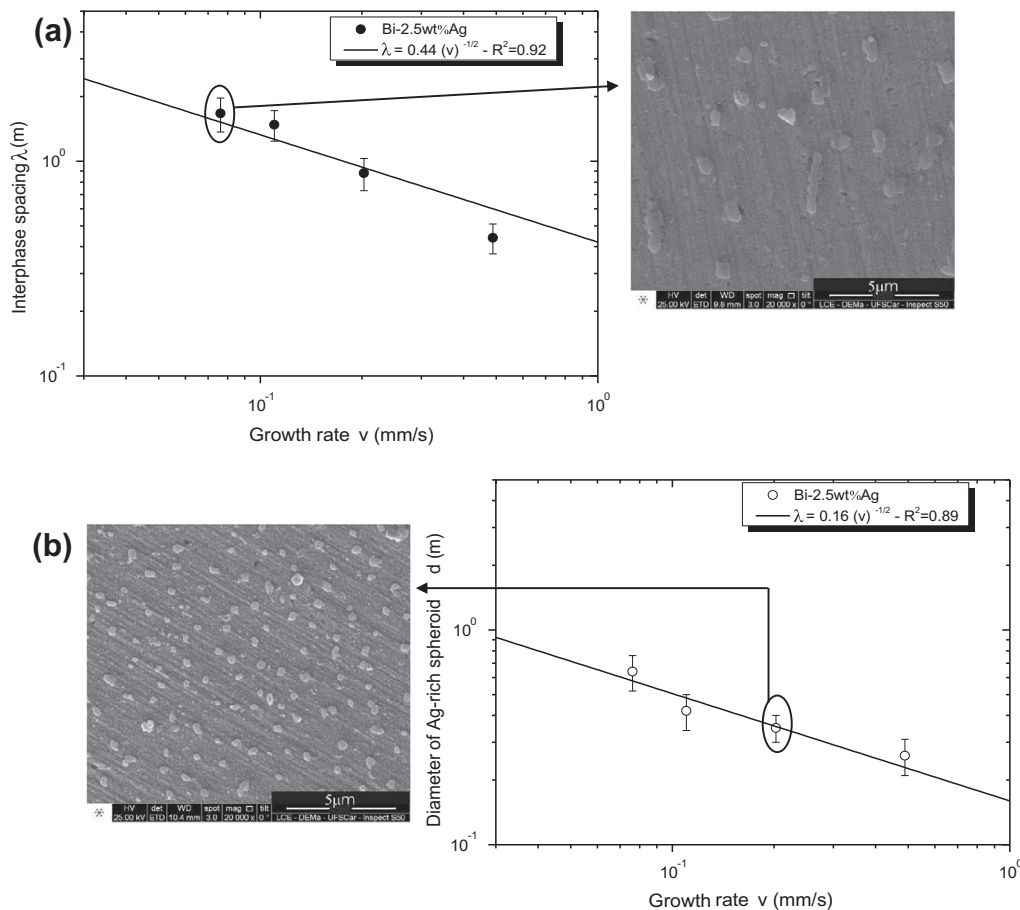


Fig. 7. (a) Interphase spacing and (b) Ag-rich spheroid diameter as a function of the growth rate for the eutectic Bi–2.5 wt%Ag solder (magnification in both SEM images of 20,000 \times). Details of the Ag spheroids are given by SEM images and arrows correlate the image with the corresponding growth rate. The digital images were acquired by SEM, in secondary electron mode. R^2 is the coefficient of determination.

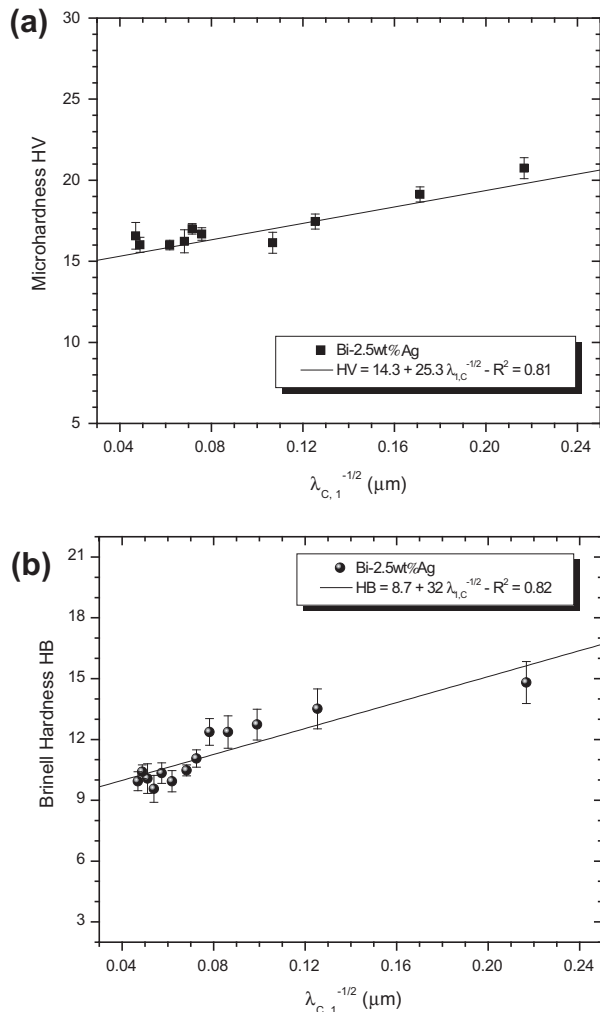


Fig. 8. (a) Vickers microhardness and (b) Brinell hardness as a function of $\lambda_{c,1}^{-1/2}$ for the Bi–2.5 wt%Ag alloy. R^2 is the coefficient of determination.

that for higher λ_1 values ($\lambda_1^{-1/2} < 0.08$) the hardness stabilizes around 16HV or 10HB. The presence of coarser and worse distributed Bi particles associated with very coarse eutectic cells may explain such steady stage in hardness.

The eutectic growth depends on the solidification conditions and for high cooling rates, small intercellular/interdendritic spacings are expected to occur as can be seen in Fig. 7. Lower spacings allow a more extensive distribution of the Ag-rich spheroids. If these soft particles are better distributed throughout the eutectic mixture, higher hardness can be expected since the eutectic Bi-rich phase will be better distributed either. The prevalence of fine Bi-rich dendrites filled with an extremely fine eutectic mixture in the very first regions of the solidified Bi–Ag casting resulted in the highest hardness values of about 21HV and 15HB.

4. Conclusions

The following conclusions can be drawn from the present experimental study:

- The non-equilibrium microstructure of the Bi–2.5 wt%Ag alloy casting is shown to be characterized by dendrites for regions close to the bottom of the casting, i.e., for growth rates (v) higher than 0.50 mm/s, followed by an abrupt cellular to dendritic transition and prevalence of eutectic colonies up to the top of the casting. For $v < 0.11$ mm/s, small Bi-rich particles

occur disseminated along the cells boundaries throughout the microstructure. These Bi particles show internal branching and faceted contours, i.e., characteristics of a faceted growth from the melt, which is in disagreement with some studies reported in the literature.

- The average eutectic cell spacing is found to vary between 113 μm and 351 μm and the average interphase spacing, associated with the presence of Ag-rich spheroids in the eutectic colonies, occurred in the range 0.4–1.7 μm . The cell spacing and primary dendrite arm spacing have been correlated with the cooling rate and the growth rate by experimental power laws characterized by -0.55 and -1.1 exponents, respectively. The eutectic interphase spacing is shown to grow following the classical eutectic growth law proposed by Jackson and Hunt, with a power function exponent of $-1/2$.
- Hall–Petch type equations are proposed relating both Vickers microhardness and Brinell hardness to the cellular/dendritic spacings. The alloy hardness is shown to increase with the decrease in the primary dendritic arm spacing or cell spacing, tending to stabilize for coarser cell spacings ($>150 \mu\text{m}$).

Acknowledgements

The authors acknowledge the financial support provided by FAPESP (São Paulo Research Foundation: grant 2013/13030-5) and CNPq (The Brazilian Research Council).

References

- [1] Normann RA. First high-temperature electronics products survey. California: Sandia National Laboratories; 2005.
- [2] Zeng G, McDonald S, Nogita K. Development of high-temperature solders: review. *Microelectron Reliab* 2012;52:1306–22.
- [3] Leinenbach C, Valenza F, Giuranno D, Elsener HR, Jin S, Novakovic R. Wetting and soldering behavior of eutectic Au–Ge alloy on Cu and Ni substrates. *J Electr Mater* 2011;40:1533–41.
- [4] Pstruś J, Fima P, Gancarz T. Wetting of Cu and Al by Sn–Zn and Zn–Al eutectic alloys. *J Mater Eng Perform* 2012;21:606–13.
- [5] Gancarz T, Pstruś J, Fima P, Mosińska S. Thermal properties and wetting behavior of high temperature Zn–Al–In solders. *J Mater Eng Perform* 2012;21:599–605.
- [6] Kim S, Kim KS, Kim SS, Suganuma K. Interfacial reaction and die attach properties of Zn–Sn high-temperature solders. *J Electr Mater* 2009;38:266–72.
- [7] Song J, Chuang H, Wu Z. Interfacial reactions between Bi–Ag high-temperature solders and metallic substrates. *J Electron Mater* 2006;55:1041–9.
- [8] Song J, Chuang H, Wen T. Thermal and tensile properties of Bi–Ag alloys. *Metall Mater Trans A* 2007;38:1371–5.
- [9] Rettenmayr M, Lambracht P, Kempf B, Graff M. High melting Pb-free solder alloys for die-attach applications. *Adv Eng Mater* 2005;7:965–9.
- [10] Spinelli JE, Garcia A. Microstructural development and mechanical properties of hypereutectic Sn–Cu solder alloys. *Mater Sci Eng A* 2013;586:195–201.
- [11] Osório WR, Garcia LR, Peixoto LC, Garcia A. Electrochemical behavior of a lead-free SnAg solder alloy affected by the microstructure array. *Mater Des* 2011;32:4763–72.
- [12] Osório WR, Leiva DR, Peixoto LC, Garcia LR, Garcia A. Mechanical properties of Sn–Ag lead-free solder alloys based on the dendritic array and Ag₃Sn morphology. *J Alloys Compd* 2013;562:194–204.
- [13] Osório WR, Peixoto LC, Leonardo LR, Mangelinck-Noël N, Garcia A. Microstructure and mechanical properties of Sn–Bi, Sn–Ag and Sn–Zn lead-free solder alloys. *J Alloys Compd* 2013;572:97–106.
- [14] El-Daly A, Hammad AE, Al-Ganainy GA, Ibrahim AA. Enhancing mechanical response of hypoeutectic Sn–6.5Zn solder alloy using Ni and Sb additions. *Mater Des* 2013;52:966–73.
- [15] Samsonov GV. Handbook of the physicochemical properties of the elements. New York: Springer, US; 1968.
- [16] Marayoshi S, Tomohiro Y, Kunio S, Hiroshi N, Tadashi T. Effects of Ag content on the mechanical properties of Bi–Ag alloys substitutable for Pb based solder. *Trans JWRI* 2012;41:51–4.
- [17] Kim JH, Jeong SW, Lee HM. Thermodynamics-aided alloy design and evaluation of Pb-free solders for high-temperature applications. *Mater Trans* 2002;43:1873–8.
- [18] Gunduz M, Çardili E. Directional solidification of aluminium–copper alloys. *Mater Sci Eng A* 2002;327:167–85.
- [19] Moura ITL, Silva CLM, Cheung N, Goulart PR, Garcia A, Spinelli JE. Cellular to dendritic transition during transient solidification of a eutectic Sn 0.7 wt%Cu solder alloy. *Mater Chem Phys* 2012;132:203–9.

- [20] Tewari N, Raj SV, Locci IE. A Comparison between growth morphology of “eutectic” cells/dendrites and single-phase cells/dendrites. *Met Mater Trans A* 2004;35:1632–5.
- [21] Song J, Chuang H, Wen T. Faceting behavior of primary Ag in Bi–Ag alloys for high temperature solder applications. *Mater Trans* 2009;50:1902–4.
- [22] Crocker MN, Fidler RS, Smith RW. The characterization of eutectic structure. *Proc Roy Soc London A* 1973;335:15–37.
- [23] Woodruff DP. *The solid–liquid interface*. Cambridge University Press; 1980.
- [24] Rosa DM, Spinelli JE, Ferreira IL, Garcia A. Cellular/dendritic transition and microstructure evolution during transient directional solidification of Pb–Sb alloys. *Metall Mater Trans A* 2008;39A:2161–74.
- [25] Jackson KA, Hunt JD. Lamellar and rod eutectic growth. *Trans Metall Soc AIME* 1966;236:1129–42.